Int J Earth Sci (Geol Rundsch) (2016) 105:1923–1940
DOI 10.1007/s00531-015-1258-z

ORIGINAL PAPER

Maximum sedimentation ages and provenance of metasedimentary rocks from Tinos Island, Cycladic blueschist belt, Greece

Tim Hinsken[1] · Michael Bröcker[1] · Jasper Berndt[1] · Claudia Gärtner[1,2]

Received: 11 May 2015 / Accepted: 1 October 2015 / Published online: 28 October 2015

Abstract U–Pb zircon ages of five metasedimentary rocks from the Lower Unit on Tinos Island (Cycladic blueschist belt, Greece) document supply of detritus from various Proterozoic, Paleozoic and Mesozoic source rocks as well as post-depositional metamorphic zircon formation. Essential features of the studied zircon populations are Late Cretaceous (70–80 Ma) maximum sedimentation ages for the lithostratigraphic succession above the lowermost dolomite marble, significant contributions from Triassic to Neoproterozoic source rocks, minor influx of detritus recording Paleoproterozoic and older provenance (1.9–2.1, 2.4–2.5 and 2.7–2.8 Ga) and a lack or paucity of zircons with Mesoproterozoic ages (1.1–1.8 Ga). In combination with biostratigraphic evidence, the new dataset indicates that Late Cretaceous or younger rocks occur on top of or very close to the basal Triassic metacarbonates, suggesting a gap in the stratigraphic record near the base of the metamorphic succession. The time frame for sediment deposition is bracketed by the youngest detrital zircon ages (70–80 Ma) and metamorphic overgrowths that are related to high-pressure/low-temperature overprinting in the Eocene. This time interval possibly indicates a significant difference to the sedimentation history of the southern Cyclades, where Late Cretaceous detrital zircons have not yet been detected.

Keywords U–Pb dating · Detrital zircon geochronology · Tinos · Cyclades · Greece

Introduction

The Attic-Cycladic crystalline belt (ACCB, Fig. 1) in the central Aegean region is a key area for the study of subduction- and exhumation-related processes. The main features of the magmatic and tectonometamorphic evolution are well documented, and geological interpretation is far advanced (e.g., Schliestedt et al. 1987; Okrusch and Bröcker 1990; Ring et al. 2010; and references therein). Not fully exploited is yet the potential of detrital zircon geochronology for characterization of the provenance and depositional history of clastic metasediments. Large parts of the ACCB are submerged below sea level, and regional correlations are severely hampered by a combination of fragmentary outcrop pattern and a complex tectonostratigraphy. Only very limited data are available for understanding the litho- and/or tectonostratigraphic framework of thick and widely distributed metasedimentary sequences. In the lower main unit of the ACCB, such sequences comprise various types of metamorphosed siliciclastic, mixed clastic-carbonate and carbonate rocks. Attempts to utilize petrographic, geochemical and isotope chemical characteristics of the marbles for regional correlations were not particularly successful (Gärtner et al. 2011). More promising is to draw the attention to the siliciclastic sediment deposits. The detrital zircon populations of these rocks can provide important information for in-depth understanding of provenance and basin development (e.g., depositional age, sediment dispersal pattern), for

Electronic supplementary material The online version of this article (doi:10.1007/s00531-015-1258-z) contains supplementary material, which is available to authorized users.

✉ Michael Bröcker
michael.broecker@uni-muenster.de

[1] Institut für Mineralogie, Westfälische-Wilhelms Universität Münster, Corrensstr. 24, 48149 Münster, Germany

[2] Institut für Geologie und Paläontologie, Westfälische-Wilhelms Universität Münster, Corrensstr. 24, 48149 Münster, Germany

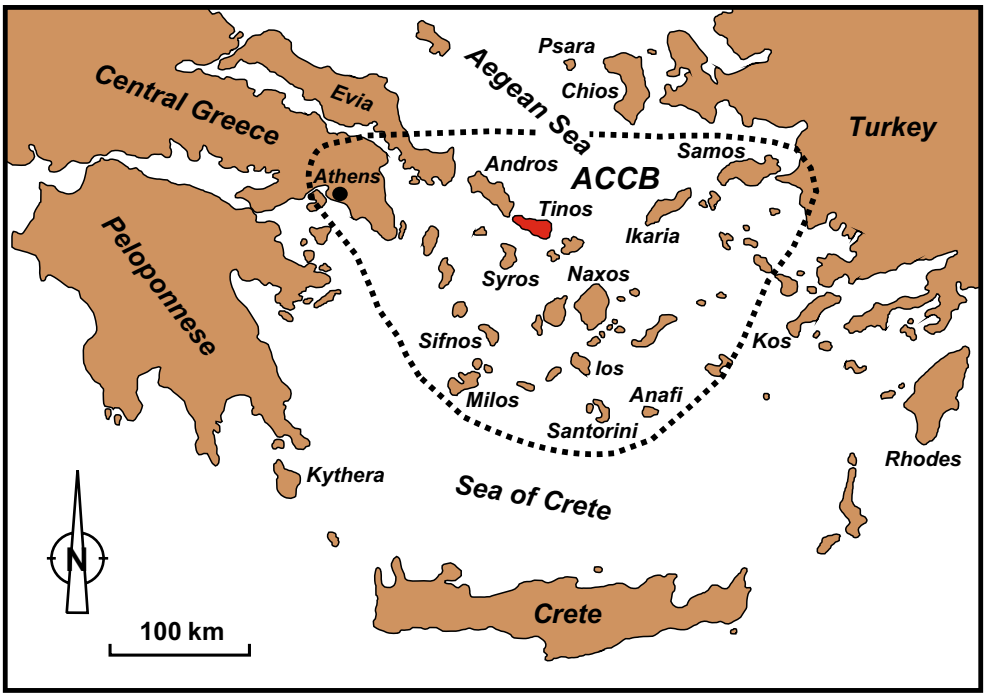

Fig. 1 Geographical overview of the larger study area. *ACCB* Attic-Cycladic crystalline belt

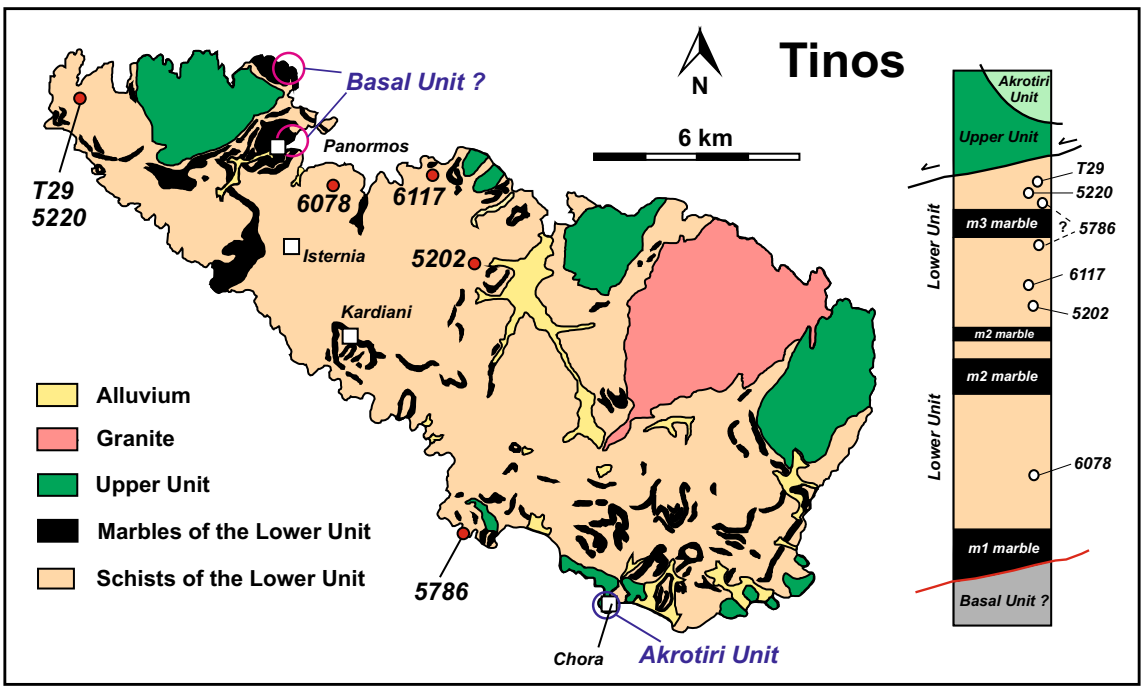

Fig. 2 Simplified geological map of Tinos (modified after Melidonis 1980) with sample locations and schematic columnar section with approximate sample positions

establishing improved regional correlations and for identification of distinct litho- and/or tectonostratigraphic units. Such data are needed to fully understand the geologic history of the larger study area.

The focus of this study is on Tinos Island (Fig. 2) where a representative segment of the ACCB is exposed in at least three tectonic subunits. We have determined detrital zircon U–Pb age spectra for metasedimentary rocks from the

Lower Unit. On a regional scale, the Lower Unit belongs to a widely distributed group of distinct tectonic slices that has been affected by Tertiary polymetamorphism, including Eocene blueschist to eclogite facies metamorphism and Oligocene/Miocene lower-pressure overprinting (e.g., Schliestedt et al. 1987; Okrusch and Bröcker 1990; Ring et al. 2010).

Our study aims at gaining more detailed knowledge of this architecture and the particular provenance and sedimentary history of the northern Cyclades. The following questions are addressed: What is the maximum depositional age recorded in the metasedimentary sequences of the Tinos Lower Unit? Is it possible to distinguish different tectonic or sedimentary subunits within this metamorphic succession? How strong is the influence of post-depositional regional metamorphism on the detrital zircon populations? Is there any evidence for contrasting depositional histories and/or provenance between Tinos and other islands of the Cycladic blueschist belt?

Geological setting

The ACCB (Fig. 1) is comprised of two major tectonic units with different *P–T–D–t* histories, each consisting of numerous fault-bounded subunits (e.g., Dürr et al. 1978; Schliestedt et al. 1987; Okrusch and Bröcker 1990; Forster and Lister 2005; Ring et al. 2010). The upper group of units is poorly preserved and comprises unmetamorphosed Permian to Mesozoic sediments, ophiolites, greenschist-facies rocks with Cretaceous to Tertiary metamorphic ages (e.g., Bröcker and Franz 1998) as well as Late Cretaceous granitoids and medium-pressure/high-temperature metamorphic rocks (e.g., Patzak et al. 1994; and references therein). Evidence for a high-pressure/low-temperature (HP/LT) stage, which is a key feature in the metamorphic evolution of the structurally lower sequences, has not been recognized. Low-angle detachments separate the upper group of units from the stack of footwall units (e.g., Avigad and Garfunkel 1989; Jolivet and Brun 2010; Jolivet et al. 2010). This structurally lower group (=Cycladic Blueschist Unit, CBU) consists of a pre-Alpine crystalline basement and volcano-sedimentary successions that include mélange sequences.

Sporadic fossils in marbles (e.g., Dürr et al. 1978; Papanikolaou 1978; Melidonis 1980) as well as U–Pb zircon dating of intercalated metavolcanic rocks (e.g., Bröcker and Pidgeon 2007), meta-igneous mélange blocks (e.g., Tomaschek et al. 2003; Bulle et al. 2010) and clastic metasedimentary rocks (Keay 1998; Löwen et al. 2015; Bröcker et al. 2015) indicate Permian to Late Cretaceous protolith ages for the cover sequences. The CBU records Eocene (*c.* 53–40 Ma) eclogite-to-epidote blueschist-facies metamorphism and subsequent overprinting at greenschist-to-upper amphibolite-facies *P–T* conditions (*c.* 25–16 Ma; e.g., Ring et al. 2010; Bröcker et al. 2013; and references therein), followed by widespread intrusion of granitoids (e.g., Altherr et al. 1982; Bolhar et al. 2010). Interpretations suggesting a prolonged Cretaceous–Eocene subduction/exhumation history (Bröcker and Enders 1999; Bröcker and Keasling 2006) have not yet been confirmed (Fu et al. 2010, 2012; Bulle et al. 2010), but are compatible with the regional geologic context.

On Tinos, a representative segment of the ACCB is exposed in at least three tectonic subunits (Fig. 2). Most of the island is part of the CBU, which is represented by the marble-schist sequence of the Lower Unit (e.g., Melidonis 1980; Bröcker et al. 1993). Remnants of HP/LT rocks are locally preserved, but pervasively overprinted rocks with greenschist-facies mineral assemblages are more common (e.g., Melidonis 1980; Bröcker et al. 1993). The whole succession can be subdivided from top to bottom by means of three mappable marble horizons (m3, m2, m1; Melidonis 1980). Variably rounded meta-igneous blocks and rock fragments (mostly <1–10 m, but up to 300 m) with Late Cretaceous U–Pb zircon ages occur widely scattered throughout the marble-schist sequence of the Lower Unit (Bulle et al. 2010).

The lowermost part of the metamorphic rock pile consists of dolomite marbles and minor phyllites that have either been interpreted as a para-autochthonous Basal Unit (Avigad and Garfunkel 1989), or as an integral part of the Lower Unit (Melidonis 1980; Bröcker and Franz 2005). In eastern Tinos (Fig. 2), a composite Miocene granitoid intrusion is exposed (*c.* 17–14 Ma; Altherr et al. 1982; Bröcker and Franz 1998) that caused contact metamorphism in both the Upper Unit and the Lower Unit (Avigad and Garfunkel 1989; Stolz et al. 1997; Bröcker and Franz 1994, 2000).

The two tectonic subunits occupying the highest structural levels (Akrotiri Unit and Upper Unit) belong to the upper main unit of the ACCB and record amphibolite- and/or greenschist-facies conditions (e.g., Patzak et al. 1994; Katzir et al. 1996; Bröcker and Franz 1998; Zeffren et al. 2005). Amphibolite-facies rocks of the topmost Akrotiri Unit yielded Cretaceous K–Ar metamorphic ages (e.g., Patzak et al. 1994). The Upper Unit (up to 500 m thick) mainly consists of metabasic phyllites, minor mica-rich phyllites and lenses and slabs (up to several hundred meters in size) of serpentinites, ophicalcites and metagabbros (Katzir et al. 1996; Bröcker and Franz 1998; Zeffren et al. 2005) that had been juxtaposed on top of the Lower Unit by an extensional detachment (e.g., Avigad and Garfunkel 1989; Katzir et al. 1996). Rb–Sr, K–Ar and $^{40}Ar/^{39}Ar$ dating documented greenschist-facies overprinting in the Miocene (Bröcker and Franz 1998; Zeffren et al. 2005). The time frame of earlier metamorphic events affecting the Upper

Unit is poorly constrained. Tectonic juxtaposition probably occurred during a regional greenschist-facies episode that also caused a pervasive overprint in the structurally lower sequences (Bröcker and Franz 1998; Zeffren et al. 2005).

Samples

The sampling strategy aimed at covering the full age range recorded by the metamorphic succession of the Lower Unit. Systematic screening showed that the number of suitable metasedimentary rocks is rather limited. Many samples do not contain zircon, or only zircon of very small grain size, making a gapless examination of the lithostratigraphic record difficult. This is especially true for the lower part of the metamorphic succession between the m2 and m1 marbles.

Six samples were selected for U–Pb geochronology. Field and/or hand-specimen pictures are shown in Fig. S1. Approximate sample locations are indicated in Fig. 2; GPS coordinates are reported in Table S2. The studied rocks include three samples (5220, 5202, T29) for which relatively small ion microprobe datasets (each comprising *c.* 35 spot analyses) were already reported by Bulle et al. (2010). These authors had specifically targeted the outermost zircon domains of individual grains to obtain constraints on the time of sediment accumulation. In order to establish robust and unbiased provenance information, we have produced additional LA-ICP-MS ages for these samples. Samples 5220, 5202 and T29 represent the main rock type ("greyschists" = graphite-bearing schists) of the clastic metasedimentary successions. Quartz, albite, white mica, chlorite and variable amounts of calcite are the dominant constituents of the mineral assemblage. Typical accessory phases are graphite, rutile, titanite, zircon, opaque phases, apatite and ±tourmaline.

Based on additional field work, three samples were newly selected. Sample 6078 is a calcschist that was collected *c.* 100 m above the m1 marble in northern Tinos, representing the lowest lithostratigraphic level dated in this study. The mineral assemblage mainly consists of calcite, quartz, feldspar, white mica and chlorite. Sample 6117 was collected in direct contact with a metaconglomeratic horizon that occurs between the m3 and m2 marbles in different parts of the island. Sample 5786 represents quartz- and feldspar-rich felsic gneisses that occur in intimately interlayered sequences with glaucophane schists (Fig. S1E, F) at a lithostratigraphic level close to the topmost m3 marble. The mineral assemblage also includes white mica, epidote/clinozoisite, chlorite and partially retrogressed blue amphibole and garnet. Titanite, zircon and opaque phases occur as accessory phases.

Analytical methods

For U–Pb geochronology, zircon was separated from ~6 to 15 kg samples by standard routines (jawbreaker, disk mill, Wilfley table, Frantz magnetic separator, methylene iodide heavy liquid, handpicking under stereomicroscope). After preparation of epoxy resin mounts and polishing to expose the grain interior, cathodoluminescence (CL) imaging was applied to reveal the internal zircon structures and to guide laser spot placement (Figs. 3, 4, 5). U–Pb geochronology was performed on a sector field ICP-MS (Element2, ThermoFisher) coupled to a 193-nm ArF Excimer laser system (UP193HE, New Wave Research) at the Institut für Mineralogie, Universität Münster. The instrument parameters for both the laser and the ICP-MS are listed in Table S1. For U–Pb analysis, the masses 202, 204, 206, 207 and 238 were measured. ^{202}Hg was analyzed to quantify the interference of ^{204}Hg on ^{204}Pb and if necessary to correct for common Pb. Corrections for laser-induced elemental fractionation, instrumental mass bias and time-dependent drift were done by bracketing groups of 10 unknowns with 3 measurements of the GJ-1 reference zircon (Jackson et al. 2004). Age calculations were carried out following the procedure described in Kooijman et al. (2012). A common Pb correction following the model of Stacey and Kramers (1975) was only applied if the contribution of the common ^{206}Pb to the total measured ^{206}Pb was 1 % or higher using the average in-run ^{204}Pb values. Data points with >5 % common Pb were rejected. The zircon grains were mostly analyzed with a laser spot diameter of ~35 μm; a small number of grains were analyzed with a ~25-μm laser spot. For U–Pb age calculations, decay constants recommended by the Subcommission on Geochronology of IUGS (Steiger and Jäger 1977) and a ^{238}U/^{235}U ratio of 137.88 were used. To monitor reproducibility and accuracy of the U–Pb ages, the 91,500 reference zircon (^{206}Pb/^{238}U = 1062.4 ± 0.8 Ma; ^{207}Pb/^{206}Pb = 1065.4 ± 0.6 Ma; Wiedenbeck et al. 1995) was analyzed and processed as an unknown yielding weighted mean ^{206}Pb/^{238}U and ^{207}Pb/^{206}Pb ages of 1065.0 ± 4.1 Ma ($n = 45$) and 1082.7 ± 8.5 Ma ($n = 46$), respectively.

Filtering of data is based on two criteria. All zircon ages were accepted that are within 90–110 % of concordance [100 × (^{206}Pb/^{238}U)/(^{207}Pb/^{206}Pb)] and, due to young ages and corresponding low precision of ^{207}Pb/^{206}Pb ratios, all data with ^{206}Pb/^{238}U and ^{207}Pb/^{235}U ages that overlap at 2-sigma uncertainty. The filtered data are reported in Table S2 as online resource. Uncertainties given for individual LA-ICP-MS U–Pb zircon analyses (ratios, ages, error ellipses) are reported with 2σ uncertainty. ^{206}Pb/^{238}U ages are quoted for analyses <1 Ga, whereas ^{207}Pb/^{206}Pb ages are quoted for analyses >1 Ga. A group of three or more overlapping analyses is considered to yield a robust

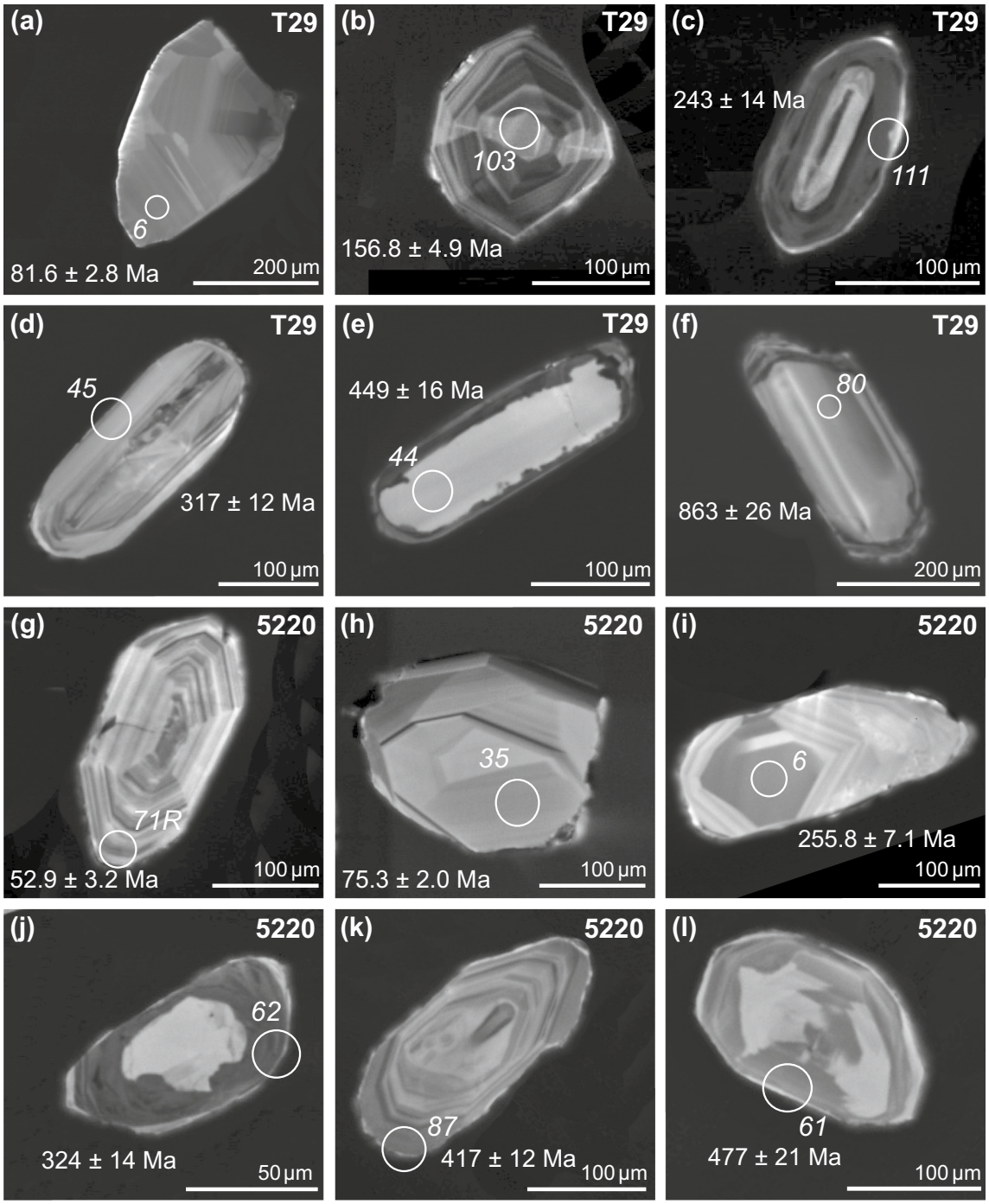

Fig. 3 Cathodoluminescence images of representative zircons of samples T29 and 5220 with $^{206}Pb/^{238}U$ ages and spot identification number. Ages are reported with 2σ uncertainty

age constraint (Gehrels 2011). Data evaluation and presentation in diagrams are based on Isoplot/Ex 3.41b (Ludwig 2005) and/or analysis tools available from www.geo.arizona.edu/alc. Histograms and probability distribution diagrams are depicted in Figs. 6, 7, 8, S4. Concordia diagrams are shown in Figs. S2, 3.

Results

Zircon characteristics and U–Pb zircon ages

Individual samples are described in descending order from top to the base of the metamorphic succession (Fig. 2).

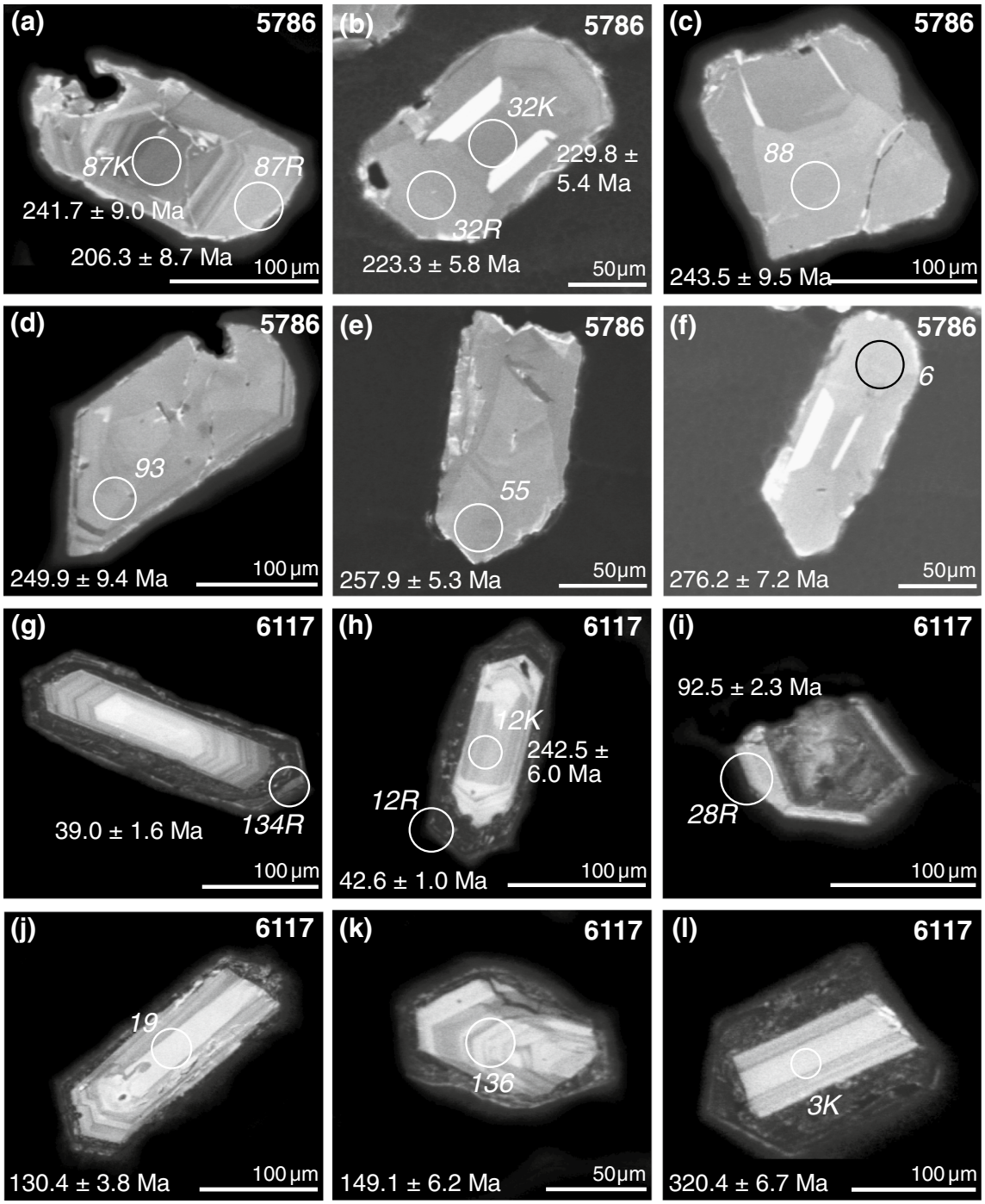

Fig. 4 Cathodoluminescence images of representative zircons of samples 5786 and 6112 with $^{206}Pb/^{238}U$ ages and spot identification number. Ages are reported with 2σ uncertainty

The mostly colorless and transparent, subhedral zircons of sample T29 show a range of internal textures that include sector-zoned, oscillatory, broad or diffuse growth zoning (Fig. 3a–f). Few grains show distinct xenocrystic core–rim relationships. More common are thin overgrowths that mantle textural discontinuities. The filtered U–Pb data (102 out of 171 spots) show an age distribution from 60 Ma to 2.65 Ga. Six data points fall in the range between 70 and 80 Ma (weighted average 78.2 ± 3.0, MSWD = 3.2). A major age population shows up in the interval between 225 and 475 Ma with several not well-developed peaks at 240–280, 290–320, 350–395 and 515–550 Ma (Fig. 6a). The

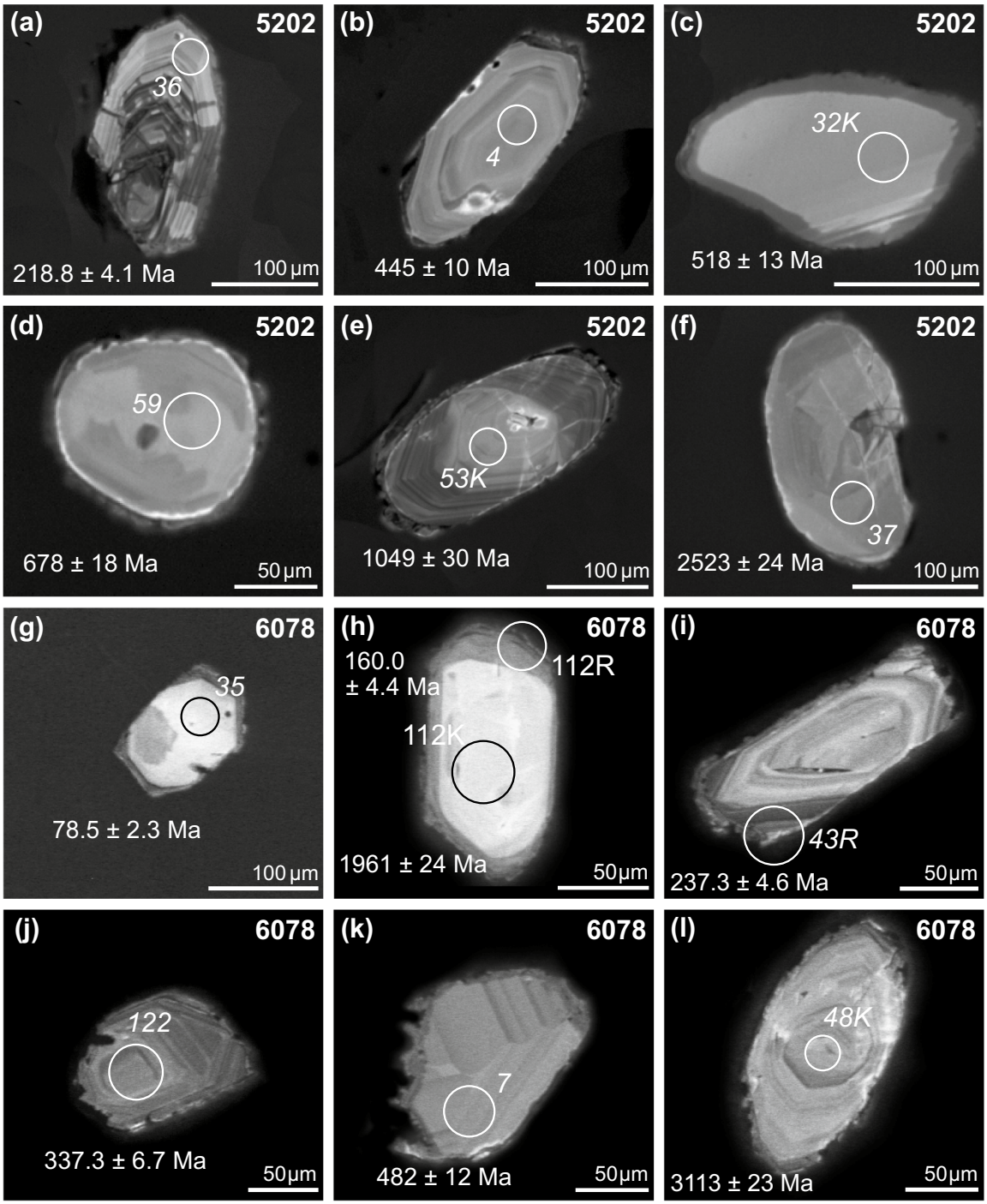

Fig. 5 Cathodoluminescence images of representative zircons of samples 5202 and 6078 with $^{206}Pb/^{238}U$ (<1000 Ma) or $^{207}Pb/^{206}Pb$ (>1000 Ma) ages and spot identification number. Ages are reported with 2σ uncertainty

most pronounced peak occurs at 420–460 Ma. Older components ($n = 6$) mostly fall into the 2.0–2.6 Ga interval.

Zircons of sample 5220 are colorless and clear, mostly subhedral crystals with concentric growth zones, sector zoning or diffuse domains. Xenocrystic cores occasionally are present (Fig. 3g–l). The analyzed zircons yielded an array of ages stretching from *c.* 50 Ma to *c.* 2.5 Ga ($n = 124$ out of 171 spots). The youngest age group ($n = 3$) occurs at *c.* 55 Ma (weighted average 54.2 ± 6.6 Ma, $n = 3$, MSWD = 3). A larger group of analyses in the range from 70 to 90 Ma permits extraction of a TuffZirc age of 83.5 +1.9/−2.7 Ma ($n = 7$, 98.4 % confidence level). Most of

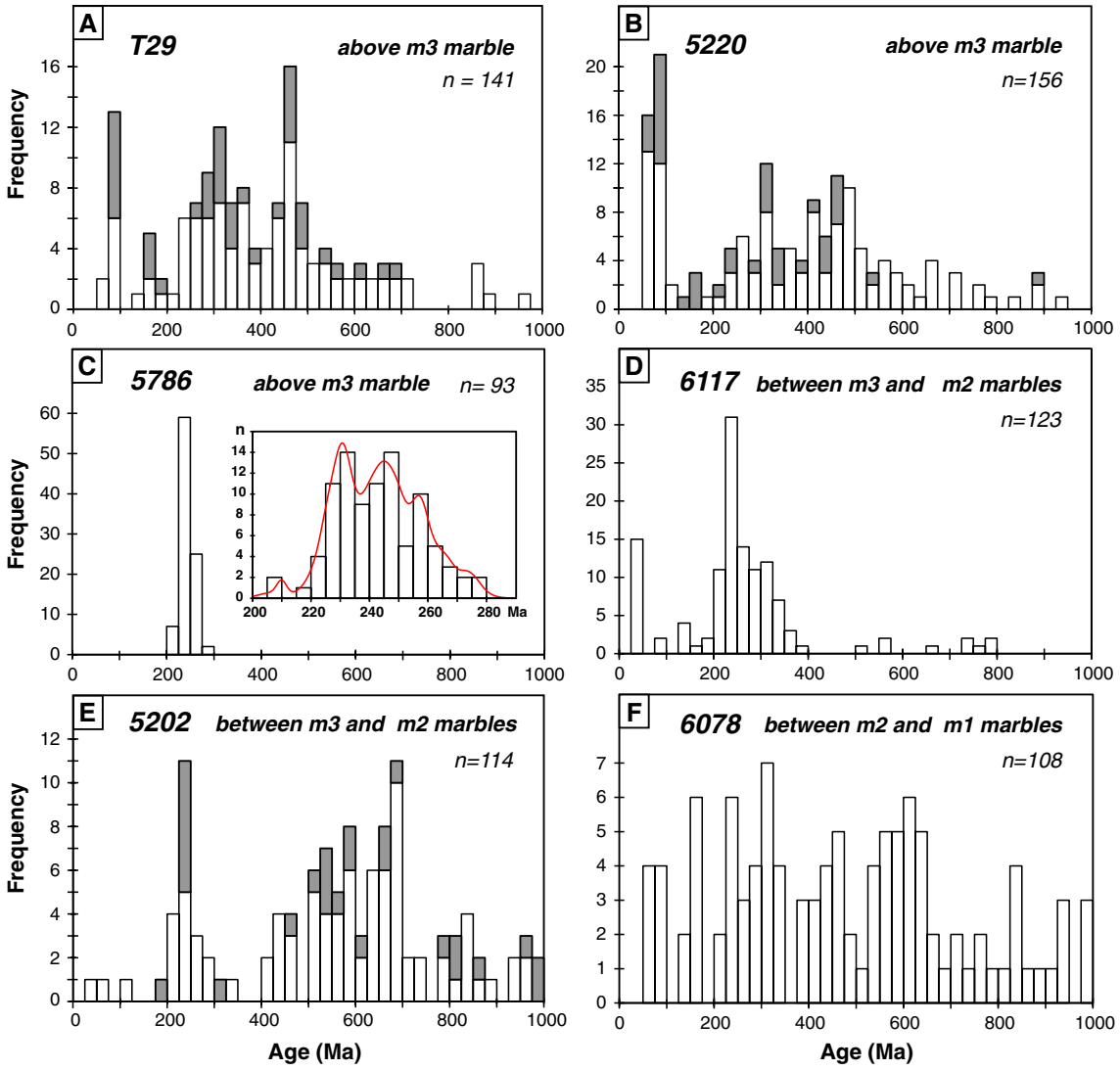

Fig. 6 Histograms showing zircon data <1000 Ma of metasedimentary rocks from the Lower Unit on Tinos. Bin width = 25 Ma. *Gray filled rectangles* indicate data of Bulle et al. (2010). *Inset* in **c** shows details of the Permian–Triassic age distribution of sample 5786 (bin width = 5 Ma)

the other data points belong to a group scattering between 225 and 710 Ma with minor peaks around 300, 340–375, 420, 465–495, 550–590 and 660 Ma (Fig. 6b).

The zircon population of sample 5786 consists of blocky to short-prismatic, sub- to euhedral, transparent grains with mostly sector-zoned, weak oscillatory-zoned or almost homogeneous textures (Fig. 4a–f). No distinct core–overgrowths relationships were recognized. The age spectrum includes 93 out of 114 analyses. All data points are integrated within a relatively narrow Triassic-Permian age population (200–275 Ma) that includes peaks around 230, 245 and 255 Ma (Fig. 6c).

Zircons of sample 6117 are euhedral to subhedral, often prismatic grains with oscillatory, sector-zoned, banded or chaotic internal structures (Fig. 4g–l). Many grains have volumetrically large overgrowths (up to 80 μm thick) with blurred and patchy internal structures. The filtered U–Pb ages ($n = 127$ out of 171 spots) range from *c.* 30 Ma to *c.* 2.6 Ga with a major population between 210 and 370 Ma (Figs. 6d, S4d). The youngest ages occur at the 40–50 Ma interval (Isoplot TuffZirc age 46 ± 1 Ma, 94 % confidence, $n = 5$). The most pronounced peak shows up at *c.* 230 Ma (Isoplot TuffZirc age 232 ± 2 Ma, 97 % confidence, $n = 23$). A minor peak is found at *c.* 300 Ma (Isoplot TuffZirc age 307 +4/−8 Ma, 98 % confidence, $n = 13$).

Zircons of sample 5202 are variably rounded grains with oscillatory, sector-zoned or faint and broad zoning that occasionally are mantled by thin, CL-dark rims (Fig. 5a–f). Few grains have distinct xenocrystic cores. The filtered U–Pb data ($n = 123$ out of 171 spots) indicate an age spectrum

from 30 Ma to 2.7 Ga. Most data points fall into the range from 400 to 700 Ma with a marked peak at 665–695 Ma (Fig. 6e). The youngest age group occurs at *c.* 220 Ma, followed by a second Triassic group at *c.* 236 Ma (Isoplot TuffZirc age 236 +2/−8 Ma, 94 % confidence, $n = 5$; weighted average: 235 ± 3 Ma, MSWD = 1.2, probability = 0.29). Thirty-six analyses yielded ages in the interval of 1.0–2.75 Ga with small peaks at *c.* 1.05, *c.* 1.95 and *c.* 2.45–2.55 Ga.

Zircons of sample 6078 show a range of subhedral to variably rounded shapes and often have a graphitic coating, as also observed for samples 5202 and 6117. The internal structures include oscillatory-, sector-zoned, faint or largely homogeneous types (Fig. 5g–l). Only few grains show distinct core–rim relationships. Some grains have very thin overgrowths. Filtered data (129 out of 171 analyses) yielded an age distribution from *c.* 64 Ma to *c.* 3.1 Ga with a high number of Paleozoic and Neoproterozoic zircons. The age spectrum shows a broad and fairly homogeneous distribution with most data points between 160 and 625 Ma. Not very well-pronounced peaks that grade into one another occur at 150–160, 230–260, 300–340, 385–440, 445–485 and 550–660 Ma (Fig. 6f). Twenty-one analyses yielded ages in the interval of 1.5–3.1 Ga with minor peaks at *c.* 2.0 and *c.* 2.6 Ga. The youngest age groups ($n = 3$) occur at *c.* 65 and *c.* 77 Ma.

Discussion

The age characteristics of the Tinos samples (Figs. 6, 7, S4) document variable degrees of denudation and/or recycling of Proterozoic, Paleozoic and Mesozoic source rocks as well as post-depositional metamorphic zircon formation. The range of detrital zircon morphologies indicates low-to-moderate textural maturity and documents both incorporation of detritus derived from nearby source areas and influx of material recording long-distance transport and/or multiple recycling. Most samples yielded a very heterogeneous polymodal U–Pb age distribution (Figs. 6, S4). The individual age spectra are rather complex and mostly lack very well-developed age peaks. Intersample similarities are not clearly recognizable. One of the studied samples is characterized by a rather restricted Triassic-Permian age range. In the following paragraphs, details of the age record, from young to old, are outlined.

U–Pb zircon ages related to in situ metamorphic processes

In all samples, a part of the zircon population is rimmed by overgrowths of variable thickness that often are too thin for meaningful U–Pb analysis. A notable exception is sample 6117 where many crystals are mantled by thick zones (up to 80 μm) of newly grown zircon, that mostly yielded Eocene (40–50 Ma) ages. Eocene ages (52–57 Ma) were also determined for three overgrowths of sample 5220; a single spot analysis of sample 5202 indicates an apparent age of *c.* 31 Ma. Taken together this group represents the youngest ages that were determined in the samples from Tinos. These ages closely correspond to Rb–Sr and Ar–Ar data reported for HP/LT and variably overprinted rocks from Tinos and other Cycladic islands (Bröcker et al. 1993, 2013; and references therein) and can be correlated with regional metamorphic processes affecting the Cycladic blueschist belt in Tertiary time. No geochronological evidence for zircon growth associated with a regional Early Miocene greenschist event (*c.* 16–23 Ma) was recognized.

Bulle et al. (2010) reported Eocene U–Pb ages (*c.* 57 Ma) for oscillatory-zoned zircon domains that are not related to distinct overgrowths and suggested that these crystals indicate either new growth of complete zircon grains during the HP/LT event or an extremely young depositional age. For two reasons, the latter interpretation cannot a priori be ruled out. Firstly, multi-method geochronological evidence indicates that an active subduction system still existed in Eocene time, implying that ocean closure was not completely finalized at this stage. Secondly, extremely fast subduction and exhumation is not an unrealistic scenario and has repeatedly been documented at convergent plate boundaries (e.g., Baldwin et al. 2004; Agard et al. 2009). It should also be kept in mind that oscillatory zoning is not an unambiguous indication for crystallization from a melt, but can as well be expected in case of precipitation from aqueous fluids, and has repeatedly been described from metamorphic phases such as garnet or clinopyroxene (Bulle et al. 2010; and references therein). At this point this question cannot conclusively be answered, but we are very skeptical toward an interpretation suggesting the presence of Late Paleocene/Early Eocene detrital zircons in the Tinos metasediments. We consider an in situ metamorphic origin of such zircon domains as a more plausible explanation. The formation of relatively thick Eocene zircon overgrowths (up to 80 μm) around unambiguous detrital grains in sample 6117 documents that favorable conditions for low-temperature (<500 °C) zircon formation locally existed at least in some metasedimentary rocks. The geological significance of data points in the range from 62 to 68 Ma remains unclear inasmuch as beam overlap on neighboring growth zones or Pb loss cannot be completely ruled out.

Maximum age of sediment deposition

The age of sediment deposition is bracketed by the youngest detrital zircons and the age of the earliest metamorphic overprint (Eocene). The youngest unequivocal detrital age

group (*c.* 70–80 Ma) underlines the importance of Late Cretaceous or younger sedimentation and had already been recognized in the less comprehensive ionprobe study of samples 5220 and T29 from the topmost part of the metamorphic succession (Bulle et al. 2010). Such ages were also detected in sample 6078 ($n = 4$) that was collected in the lower segment of the metamorphic rock pile. A single spot age of *c.* 71 Ma was determined in sample 5202 representing an intermediate stratigraphic position. This age distribution suggests that sediment accumulation recorded in the complete schist sequence of the Lower Unit took place at least until Late Cretaceous time. There is no indication for a marked vertical age gradient through the lithostratigraphic succession (*c.* 1250–1800 m).

It is not really surprising that Late Cretaceous detrital ages were also found in the lowermost part of the metamorphic succession. This outcome was almost predictable. Variably rounded blocks and rock fragments occur widely scattered in the marble-schist sequence of the Lower Unit, but mostly in the upper part of the lithostratigraphic succession (Bulle et al. 2010). These blocks most likely represent recycled fragments of oceanic lithosphere that accumulated after slope failure in an olistostromatic deposit (Bulle et al. 2010). All yet dated blocks yielded a single U–Pb age group of *c.* 80 Ma and zircons with corresponding ages were also reported from the enclosing matrix rocks (Bulle et al. 2010). A mélange sequence is also exposed close to the lowermost m1 calcite marble near Panormos (Bulle et al. 2010). In analogy to similar occurrences at higher lithostratigraphic level, a related origin and mode of formation can reasonably be expected. Although no geochronological data are yet available for any mélange block from the Panormos area, a Late Cretaceous age is very likely. The Late Cretaceous or younger depositional age of sample 6078, representing a block-free metasediment layer from the lower segment of the Tinos metamorphic succession, is in accordance with this hypothesis.

Provenance of Late Cretaceous zircons

The Tinos block-matrix association includes Late Cretaceous source rocks and is either of olistostromatic origin or related to intraoceanic brecciation and reworking (Bulle et al. 2010), but in any case derived from a nearby located source area, as indicted by the well-preserved morphology of such zircon crystals in the schists. Late Cretaceous U–Pb zircon ages have also been reported for meta-igneous mélange blocks from Syros and Samos (Keay 1998; Tomaschek et al. 2003; Bröcker and Keasling 2006; Bröcker et al. 2014). For these occurrences, correlative relationships between each other (e.g., Candan et al. 1997) and with the mélange on Tinos have been suggested (Bröcker et al. 2014). Elsewhere in the larger region, similar U–Pb zircon ages were described from some meta-ophiolite occurrences that are exposed along the Inner Tauride suture zone in Turkey (88.8 ± 2.5, 82.8 ± 4.0, 69.1 ± 2.1 Ma; Parlak et al. 2013), albeit somewhat older protolith ages (*c.* 90–95 Ma) apparently characterize the majority of the Turkish meta-ophiolites (e.g., Parlak and Delaloye 1999).

Paleocene to Late Cretaceous ages of high-temperature/low-pressure metamorphic rocks (K–Ar and Rb–Sr ages *c.* 60–84 Ma) and associated granitoid intrusions (U–Pb zircon ages *c.* 74–85 Ma) were also reported from the Upper Unit of the ACCB (e.g., Anafi, Tinos, Ikaria) and from Crete and were interpreted to represent remnants of the Asteroussia nappe (e.g., Reinecke et al. 1982; Patzak et al. 1994; Altherr et al. 1994; Langosch et al. 2000; Be'eri-Shlevin et al. 2009; Kneuker et al. 2015). Furthermore Late Cretaceous U–Pb ages (76–92 Ma) are known from felsic igneous rocks of the Sredna Gora belt in Bulgaria (von Quadt et al. 2005) and some granitoids of the Serbo-Macedonian Massif (68–63 Ma, Himmerkus et al. 2012). However, contributions of detritus from these source terrains are considered unlikely, due to the meta-ophiolitic nature of the Cycladic mélange blocks and the associated matching characteristics of zircons from their schist matrix.

Other Mesozoic and Late Paleozoic ages

The Tinos detrital zircon population also documents sediment supply from Early Cretaceous and Jurassic terrains. Potential source rocks for Early Cretaceous zircons are exposed in the Pelagonian Zone in northern Greece from where Schenker et al. (2014) reported U–Pb zircon ages of *c.* 100–130 Ma for migmatitic rocks. A similar protolith age (117.4 ± 1.9 Ma) was determined for an UHP rock of the Rhodope zone (Liati et al. 2002; Liati 2005). Based on Pb–Pb and U–Pb zircon dating, several studies have documented somewhat older Early Cretaceous to Late Jurassic ages for metagranitic rocks of the Rhodope region (*c.* 134–164 Ma; Turpaud and Reischmann 2010; Liati et al. 2011; Bonev et al. 2015), the Pelagonian Zone (*c.* 137 Ma, Anders et al. 2007), the Vardar Zone (*c.* 155–164 Ma; Anders et al. 2005) and the Serbo-Macedonian Massif (*c.* 140–156 Ma; Himmerkus et al. 2012). A distinct (U)HP stage of the polyphase tectonometamorphic evolution of the Rhodope Massif also falls within this age range (*c.* 149 Ma, U–Pb zircon, Liati 2005). The widely distributed remnants of Jurassic ophiolites that are exposed across large parts of the Balkan (e.g., Robertson 2002) locally comprise volumetrically subordinate amounts of zircon-bearing rock types that mostly yielded Jurassic ages (*c.* 169–173 Ma, Liati et al. 2004; *c.* 156–160 Ma, Bröcker and Pidgeon 2007) with presumably small contribution to the detrital record.

During Triassic and Late Paleozoic times the eastern Mediterranean region experienced major episodes of granitoid intrusions (e.g., Keay 1998; Koralay et al. 2001; Engel and Reischmann 1998; Reischmann 1998; Vavassis et al. 2000; Reischmann et al. 2001; Photiades and Keay 2003; Turpaud and Reischmann 2010; Bröcker and Pidgeon 2007; Okay et al. 2001, 2006; Xypolias et al. 2006; Anders et al. 2007; Lode et al. 2008; Himmerkus et al. 2009a; Liati et al. 2009, 2011, 2013; Chatzaras et al. 2013; Fu et al. 2015). The geodynamic context of the Triassic igneous activity is controversially discussed and has either been related to subduction- or to rifting-related processes (for a detailed discussion, see Chatzaras et al. 2013; and references therein). For the Carboniferous-Permian magmatic phase (*c.* 320–280 Ma), a relationship to the closure of the Paleotethys is generally accepted (e.g., Pe-Piper and Piper 2002; and references therein). Zircons with correlative ages to the Triassic and Carboniferous-Permian magmatic episodes represent essential components of the detrital populations from Tinos. In many cases, almost euhedral crystals indicate short transportation distances and influx from nearby sources, but both age groups may include detritus of faraway provenance. In the Cyclades, present-day outcrops of Triassic meta-igneous rocks have been described, for example, from Syros, Andros and Ios (Keay 1998; Tomaschek et al. 2003; Bröcker and Pidgeon 2007; Fu et al. 2015). Carboniferous-Permian basement rocks have been identified on Naxos, Paros, Sikinos, Ios, Delos and Syros (Henjes-Kunst and Kreuzer 1982; Engel and Reischmann 1998; Reischmann 1998; Keay et al. 2001; Tomaschek et al. 2008).

Paleozoic and Precambrian ages

A prominent age population shows up between 350 and 700 Ma with several minor peaks and a maximum at *c.* 450 Ma (Fig. 7) that had already been recognized in samples from other Cycladic occurrences (Keay and Lister 2002). Data points at the younger end of this age group document influx of detritus from Devonian sources. Igneous and meta-igneous rocks with such U–Pb zircon ages have been reported, for example, from various islands of the Cyclades (*c.* 370–413 Ma; Keay and Lister 2002) and the Biga peninsula, NW Turkey (*c.* 398 Ma; Okay et al. 2006).

The Late Neoproterozoic to Paleozoic segment of the age spectrum includes the major igneous age peaks at 440, 560 and 700 Ma reported from parts of the Serbo-Macedonian Massif and the Pelagonian Zone (Florina terrane) that are considered to represent exotic Gondwana-related terranes within the Internal Hellenides (e.g., Anders et al. 2006, 2007; Himmerkus et al. 2006, 2007; and references therein). The Neoproterozoic to Cambrian ages (*c.* 500–700 Ma) can broadly be related to Pan-African/Cadomian igneous sources that have been reported from several occurrences in Bulgaria, Greece and Turkey (e.g., Meinhold et al. 2008; and references therein). The Ordovician–Silurian peak that slightly stands out from the main data accumulation of the Tinos samples largely corresponds to ages of the Vertiskos terrane in the NW part of the Serbo-Macedonian Massif (410 and 450 Ma) and similar ages reported from SW Bulgaria and the Biga Peninsula in NW Turkey (e.g., Himmerkus et al. 2006, 2007; Meinhold et al. 2009, 2010; and references in these papers).

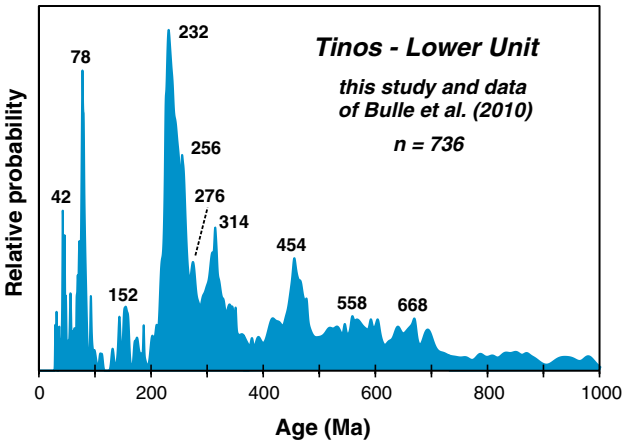

Fig. 7 Probability distribution diagram with peak ages showing compilation of zircon data <1000 Ma for all Tinos samples, including data reported by Bulle et al. (2010)

The age record of the Tinos samples includes minor peaks at 0.9–1.1, 1.95–2.1, 2.4–2.55 and 2.6–2.7 Ga (Fig. S4). The small number or complete lack of detrital zircons with ages between 1.1 and 1.8 Ga has repeatedly been documented in various parts of the Hellenides, Pontides and Taurides and, in combination with the presence of 2 Ga old zircons, has been interpreted to indicate the influx of sediment with northern Gondwanan provenance (e.g., Keay and Lister 2002; Himmerkus et al. 2007, 2009b; Meinhold and Frei 2008; Meinhold et al. 2008, 2010; Ustaömer et al. 2012; Kydonakis et al. 2014; Zlatkin et al. 2013; Abbo et al. 2015; Dörr et al. 2015). The data from Tinos show great similarity with age distribution patterns of the larger Aegean region that indicate a relationship to North African-derived sources (e.g., Kröner and Sengör 1990; Keay and Lister 2002; Avigad et al. 2003; Zulauf et al. 2007; Ustaömer et al. 2012; Marsellos et al. 2012; Kydonakis et al. 2014). These occurrences represent large volumes of sedimentary rocks incorporating detritus derived from various parts of the East African orogen (Transgondwanan Supermountain) and Saharan Metacraton (Meinhold et al. 2013; Kydonakis et al. 2014; Avigad et al. 2015). The age distribution patterns reported from Tinos and other parts

of the Cyclades (Keay and Lister 2002) allow a clear distinction from other peri-Gondwanan terranes with Avalonian- or Amazonian-type affinity that have been identified on mainland Greece and in NW Turkey (e.g., Anders et al. 2006, 2007; Ustaömer et al. 2011; Zlatkin et al. 2014).

Samples with localized provenance record

The maximum age of sediment deposition for the Tinos Lower Unit, as constrained by the youngest detrital age groups of samples from the topmost part and the lower segment of the metamorphic succession, is not recorded in the age distribution patterns of samples 5786 and 6117 (Fig. 6c, d). Sample 6117 was collected between the m3 and m2 marble horizons and represents a relatively thin layer (up to *c.* 2 m in thickness) of a conglomeratic to pebbly calcschist. Compared to most other Tinos samples, the detrital age spectrum is rather restricted, mostly in the 200–350 Ma range, with only few data points >400 Ma. The determining factors controlling the composition of the zircon population of samples 5786 and 6117 (e.g., rates of sediment supply, specific transport and accumulation processes, degree of mixing) are obviously different from those of the siliciclastic and/or calcite-rich metasedimentary rocks that dominate the Tinos succession, causing a natural bias of the detrital age record.

Sample 5787 was collected in the upper part of the Lower Unit at a lithostratigraphic level close to the m3 marbles and represents an outcrop of felsic rocks and blueschists that are interlayered on the several decimeter-scale. Within a short distance to this outcrop an eclogitic mélange block is exposed, but available field observations provide no convincing indications (e.g., ultramafic selvages as observed at other block-matrix contacts) that the intercalated blueschist-gneiss rocks may also represent an exotic tectonic slice. Other occurrences of this rock association are found in the northern part of the island in a comparable lithostratigraphic position and most likely represent a distinct volcano-sedimentary horizon within the original succession. Similar rocks, interpreted to represent a bimodal volcanic rock association, have been described from the neighboring island of Syros, where they occur as part of the main marble-schist sequence (Tomaschek et al. 2003) and as a large tectonic slab within the northern mélange belt (Bröcker and Keasling 2006). On Syros, U–Pb dating of zircon from the felsic rocks yielded well-constrained Triassic ages (243 ± 2, 240.1 ± 4.1 and 245.3 ± 4.9 Ma; Tomaschek et al. 2003; Bröcker and Keasling 2006). Despite some field and petrographic similarities, the intercalated blueschist-gneiss rocks from Tinos are different to the Syros occurrences. Instead of meta-igneous precursors, on Tinos the felsic layers most likely represent immature quartzofeldspathic metasandstones. U–Pb zircon data of sample 5786 yielded a Triassic to Permian age spectrum indicative of a metasedimentary rock with a strongly localized provenance. Well-preserved zircon crystals indicate derivation from nearby source rocks. The youngest age group indicates a maximum depositional age around 220 Ma. Quartz-rich metasediments with zircons that show little evidence of transport and a rather restricted, mostly Triassic provenance have also been reported from Naxos (Keay 1998) and Syros (Löwen et al. 2015). In this context worth mentioning are also quartz- and feldspar-rich samples from Ios that mainly yielded either Triassic (*c.* 245 Ma) or Late Paleozoic (*c.* 280–320 Ma) U–Pb zircon ages (Fu et al. 2015), and a felsic sample from a interlayered sequence of meta-acidic rocks and greenschist on Sifnos that mainly yielded Triassic ages (*c.* 220–240 Ma; Bröcker and Pidgeon 2007). These samples were interpreted to represent metatuffaceous rocks. However, identification of the protolith of metafelsic rocks is often ambiguous and these rocks might also represent immature metasandstones with a strongly localized provenance.

The Tinos metasedimentary sequences document episodic influx of material derived from different sources. The whole succession most likely represents deposits of mixed siliciclastic-carbonate turbidity currents that alternate with pure carbonate turbidites (e.g., Bröcker and Franz 2005). Conglomeratic layers and dispersed blocks of meta-igneous rocks indicate occasional contributions of submarine slides. The restricted provenance of some layers documents shorter cycles of sediment accumulation and a lesser degree of mixing before final deposition than recorded in the adjacent schist sequences.

Age constraints for missing section in the stratigraphic record

The lowermost part of the metamorphic succession on Tinos is exposed around the village of Panormos (Fig. 2; Melidonis 1980; Avigad and Garfunkel 1989). In this area, the rock pile is dominated by well-layered calcite-rich marbles which are underlain by massive dolomite marbles and minor phyllites. From the dolomites, Melidonis (1980) reported findings of Upper Triassic (Norian–Rhaetian) marine algae and corals. No biostratigraphic remnants are preserved in the directly overlying calcite marble or in marbles occurring at higher lithostratigraphic levels. Originally, the complete basal marble succession (=m1 marbles) was assigned to the Lower Unit (Melidonis 1980). This interpretation was questioned by Avigad and Garfunkel (1989) who interpreted the base of the calcite marbles as a structural discordancy and suggested that the lowermost sequence represents a para-autochthonous basal unit beneath the Cycladic blueschists with a distinct metamorphic and deformational history. The tectonic contact

between both units was interpreted as a thrust fault (Avigad and Garfunkel 1989). Bröcker and Franz (2005) agreed with the existence of a tectonic contact within the marbles, but related this fault to extensional processes. According to these authors, field observations, petrological and geochronological data are fully compatible with the interpretation that the dolomite-phyllite succession is an integral part of the CBU, as originally suggested by Melidonis (1980). The tectonic concept suggested by Avigad and Garfunkel (1989) bears similarities to the Olympus-Ossa region on mainland Greece and to Evia Island where fossil-bearing Triassic and Cretaceous to Early Tertiary metacarbonates are overlain by a stack of thrust sheets recording higher-grade HP/LT metamorphism than observed in the structurally lowest unit (Schermer et al. 1990; Nance 2010; Shaked et al. 2000).

The new detrital zircon data of this study indicate the existence of a significant gap in the stratigraphic record in northern Tinos. Fossil-bearing Upper Triassic dolomites (*c.* 240 Ma) at the base of the succession are overlain by Late Cretaceous (70–80 Ma) or younger schist sequences, as indicated by the maximum depositional age for a calcschist collected relatively close to the m1 calcite marble, and the presumably corresponding age of a local mélange sequence directly above the Panormos marbles. There is no evidence for an episode of subaerial exposure and erosion within the marble succession, as, e.g., indicated by the metabauxites on Naxos (Feenstra 1985).

The existence of a missing section in the stratigraphic record corroborates the concept of a tectonic contact within the basal metacarbonate sequence. However, the total age range and the thickness of the missing section remain uncertain, mainly for two reasons: (1) It is unclear which time span is covered by the undated marble-quartzite sequence (*c.* 50 m in thickness) above the dolomites. No fossils were recognized in the m1 calcite marbles, and interlayered quartzites do not contain detrital zircon. (2) The apparent biostratigraphic age of the dolomites may not be identical with the true sedimentation age, e.g., due to yet unrecognized reworking and redeposition of preexisting fossil-bearing carbonates.

The nature of the fault is difficult to assess. Missing sections are commonly associated with normal faulting, but may also be related to tectonic juxtaposition of a thrust unit. Judging from field observations and the geological context known so far, it is impossible to distinguish between a thrusting- or extension-related origin of the Panormos fault zone. The situation is further complicated by the fact that thrust faults may have experienced reactivation as normal faults during extension (e.g., Forster and Lister 2005; Huyskens and Bröcker 2014; Bröcker et al. 2015). The presumed status of the basal Panormos section as a distinct tectonic entity with a geologic and tectonometamorphic history that is different from the overlying sequences has yet not convincingly been demonstrated. This question can only be resolved if future efforts will improve understanding of the *P–T–t* history of the basal sequence and/or in case that a different provenance of the footwall sequences can unambiguously be documented.

Evidence for tectonic duplication at higher lithostratigraphic levels?

Detrital zircon ages do not directly date the time of sediment deposition, but only provide an upper limit for this process. On Tinos the youngest detrital age group (70–80 Ma) was recognized both in the topmost part of the lithostratigraphic succession and in its lower segment. An upwards younging-trend of zircon ages has not been detected. This does not necessarily imply relatively rapid accumulation of the complete Lower Unit succession (*c.* 1250–1800 m; Melidonis 1980), because the available time span indicated by the youngest detrital zircons (70–80 Ma) and the Eocene HP/LT event (*c.* 40–53 Ma) still embraces a considerable interval. Modification of the internal structure of the Lower Unit by tectonic stacking or large-scale isoclinal folding, as has been suggested for similar successions on other Cycladic islands (e.g., Forster and Lister 2005; Keiter et al. 2011), can currently not be ascertained, due to the lack of supporting field observations. For this reason, we consider it more likely that the rock sequences above the Panormos fault represent a coherent lithostratigraphic succession, deposited within no more than 30–40 myr, with a Late Cretaceous maximum sedimentation age.

Regional comparison of the detrital zircon record

A comprehensive geochronological and isotope geochemical database for detrital zircons is essential for developing an improved understanding of the depositional history and the paleogeographic setting of the Cyclades and for unraveling the litho- and/or tectonostratigraphic relationships across the larger study area. The picture emerging from available data is still fragmentary. Geochronological provenance characteristics have not yet rigorously been explored, and combined U–Pb age and Hf isotope datasets are not available at all. Figure 8 gives an overview of the Neoproterozoic and younger detrital zircon age data reported from various parts of the Cycladic blueschist belt (Keay and Lister 2002; Löwen et al. 2015; Bröcker et al. 2015, this study). The current state of knowledge can be summarized as follows:

The Makrotantalon Unit on Andros occupies a special position. Both the detrital zircon record (Fig. 8a; Bröcker et al. 2015) and differences in the timing of metamorphic overprinting (Huyskens and Bröcker 2014; Huet et al. 2015) provide evidence for the distinct nature of this tectonic unit that possibly is of Pelagonian origin (Huet et al.

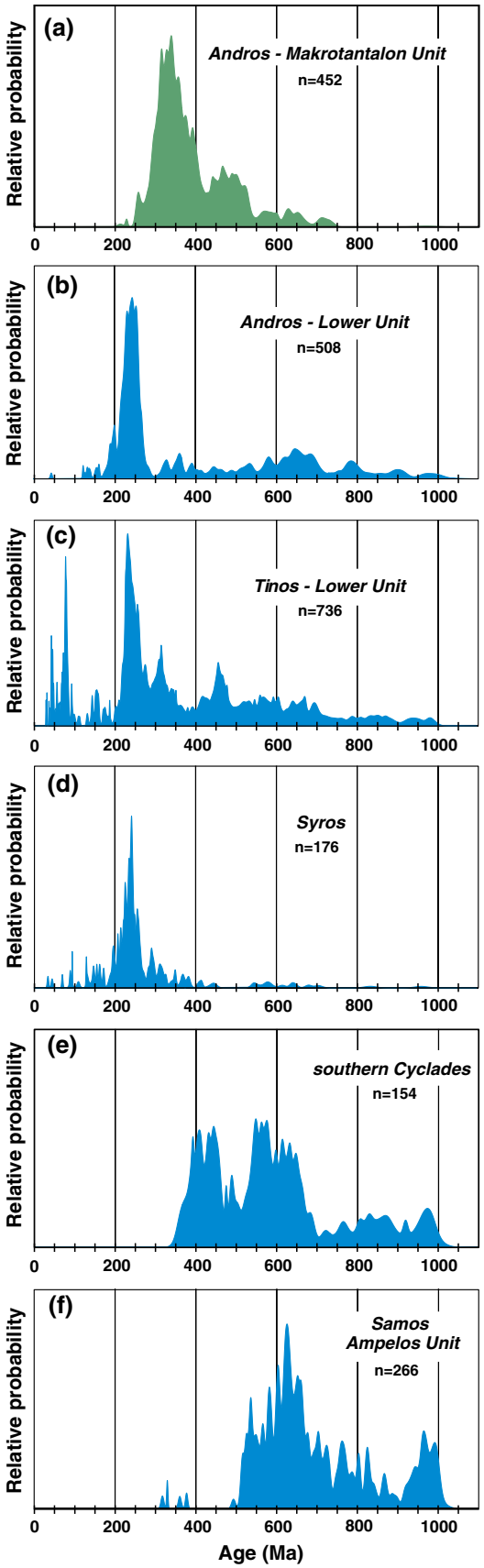

◀ **Fig. 8** Probability distribution diagrams of Neoproterozoic and younger U–Pb detrital zircon data from the larger study area. **a**, **b** Andros (Bröcker et al. 2015), **c** Tinos (this study, Bulle et al. 2010), **d** Syros (Löwen et al. 2015), **e** southern Cyclades (Keay and Lister 2002), **f** Samos (Löwen et al. 2015). *Green* Pelagonian zone, *blue* Cycladic blueschist unit. See text for further explanation

2015). The youngest detrital zircons indicate a maximum depositional age of *c.* 260 Ma (Bröcker et al. 2015).

All other datasets represent the Cycladic Blueschist Unit. It is obvious from this compilation that Late Paleozoic and Triassic igneous source rocks provided essential components for the detrital zircon populations in the northern Cyclades (Andros, Tinos, Syros; Fig. 8b–d). The apparent absence of such ages in the southern part of the archipelago (Naxos, Paros, Sifnos, Sikinos, Folegandros, Ios), as implied by Fig. 8e, is an artifact of data selection by Keay and Lister (2002) for the particular purpose of their study. The largely unpublished post-Carboniferous ages for this area also include abundant evidence for Late Paleozoic and Triassic magmatic activity (Keay 1998). The pre-Carboniferous data (Fig. 8e) suggest a North African origin for the Cycladic basement and cover sequences (Keay 1998; Keay and Lister 2002). The presence and distribution of Neoproterozoic and Paleozoic ages on Andros and Tinos are in line with this interpretation.

The paucity or lack of <500 Ma ages in the Samos samples (Fig. 8f) is in marked contrast to the data from the northern part of the Cycladic blueschist belt, but shows similarities with age distribution patterns recording the influx of "Pan-African" detritus that are common elsewhere in the eastern Mediterranean region (e.g., Löwen et al. 2015; and references therein). However, the Samos study focused on the maximum sedimentation age of a distinct lithostratigraphic level (Löwen et al. 2015) and thus cannot provide a comprehensive picture. The Andros and Syros studies aimed a covering the full age range recorded by the metamorphic succession, but also placed emphasis on unraveling maximum depositional ages (Löwen et al. 2015; Bröcker et al. 2015).

For the Tinos and Syros metasedimentary successions, a Late Cretaceous maximum depositional age is well established (this study; Löwen et al. 2015) and can be related to the same source that supplied meta-igneous mélange blocks with corresponding U–Pb zircon ages (e.g., Bulle et al. 2010; Bröcker et al. 2014). Due to the correlative field relationship between Syros, Tinos and Andros (e.g., Bulle et al. 2010; Bröcker et al. 2014, 2015), a similar depositional age can be inferred for the topmost part of the Andros Lower Unit succession. The Late Cretaceous or younger sedimentation in the northern Cyclades might indicate a significant difference to the sedimentation history of the southern Cyclades, where unambiguous detrital zircons of this

age range have yet not been recognized. Available data of Keay (1998) were interpreted to document mainly Triassic to Late Jurassic maximum depositional ages. Several age peaks falling in the range from Early to Late Cretaceous time were related to post-depositional metamorphic overgrowths (Keay 1998).

Summary and conclusions

Essential features of the new zircon dataset for metasedimentary rocks from the Lower Unit on Tinos are the presence of (1) Eocene metamorphic overgrowths related to an in situ metamorphic overprint; (2) a Late Cretaceous (70–80 Ma) maximum sedimentation age across the complete lithostratigraphic succession of the Lower Unit; (3) a relatively small number of Early Cretaceous and Jurassic ages; (4) variable but major contributions from Triassic to Neoproterozoic source rocks; (5) minor influx (<5 %) of detritus recording Paleoproterozoic and older provenance (1.9–2.1, 2.4–2.5 and 2.7–2.8 Ga) and (6) a lack or paucity of zircons with U–Pb ages in the range from 1100 to 1800 Ma. As reported from other Cycladic islands (e.g., Naxos, Syros, Ios; Keay 1998; Löwen et al. 2015; Fu et al. 2015), the Tinos metasedimentary succession sporadically contains intercalations with a strongly localized provenance.

Taken together, the detrital zircon record of clastic metasediments from Tinos substantiates the importance of Triassic and Late Paleozoic igneous sediment sources and the involvement of detritus with North African affinity (Keay 1998; Keay and Lister 2002) for the Cycladic depositional basin. The new U–Pb age data also underline the importance of Late Cretaceous (*c.* 70–80 Ma) or younger sedimentation, at least in the northern part of Cycladic blueschist belt, and suggest the existence of a significant gap in the Tinos stratigraphic record near the base of the metamorphic succession. The age of sediment deposition recorded in the Tinos Lower Unit is bracketed by the youngest detrital zircons (*c.* 70–80 Ma) and the onset of regional metamorphic overprinting (*c.* 40–53 Ma).

Acknowledgments MBR gratefully acknowledges support through the Deutsche Forschungsgemeinschaft (Grant BR 1068/17-1). Reviews by Dov Avigad and Guido Meinhold helped to clarify our presentation and are much appreciated.

References

Abbo A, Avigad D, Gerdes A, Güngör T (2015) Cadomian basement and Paleozoic to Triassic siliciclastics of the Taurides (Karacahisar dome, south-central Turkey): paleogeographic constraints from U–Pb–Hf in zircons. Lithos 227:122–139

Agard P, Yamato P, Jolivet L, Burov E (2009) Exhumation of oceanic blueschists and eclogites in subduction zones: timing and mechanisms. Earth Sci Rev 92:53–79

Altherr R, Kreuzer H, Wendt I, Lenz H, Wagner GA, Keller J, Harre W, Höhndorf A (1982) A Late Oligocene/Early Miocene high temperature belt in the Attic-Cycladic crystalline complex (SE Pelagonian, Greece). Geol Jahrb E 23:97–164

Altherr R, Kreuzer H, Lenz H, Wendt I, Harre W, Dürr S (1994) Further evidence for Late-Cretaceous low pressure/high-temperature terrane in the Cyclades, Greece. Chem Erde 54:319–328

Anders B, Reischmann T, Poller U, Kostopoulos D (2005) Age and origin of granitic rocks from the eastern Vardar Zone: new constraints on the evolution of the Internal Hellenides. J Geol Soc Lond 162:857–870

Anders B, Reischmann T, Kostopoulos D, Poller U (2006) The oldest rocks of Greece: first evidence for a Precambrian terrane within the Pelagonian Zone. Geol Mag 143:41–58

Anders B, Reischmann T, Kostopoulos D (2007) Zircon geochronology of basement rocks from the Pelagonian Zone, Greece: constraints on the pre-Alpine evolution of the westernmost Internal Hellenides. Int J Earth Sci 96:639–661

Avigad D, Garfunkel Z (1989) Low-angle faults above and below a blueschist belt—Tinos Island, Cyclades, Greece. Terra Nova 1:182–187

Avigad D, Kolodner K, McWilliams M, Persing H, Weissbrod T (2003) Origin of northern Gondwana Cambrian sandstone revealed by detrital zircon SHRIMP dating. Geology 31:227–230

Avigad D, Weissbrod T, Gerdes A, Zlatkin O, Ireland TR, Morag N (2015) The detrital zircon U–Pb–Hf fingerprint of the northern Arabian-Nubian Shield as reflected by a Late Ediacaran arkosic wedge (Zenifim Formation; subsurface Israel). Precambrian Res 266:1–11

Baldwin SL, Monteleone BD, Webb LE, Fitzgerald PG, Grove M, Hill EJ (2004) Pliocene eclogite exhumation at plate tectonic rates in eastern Papua New Guinea. Nature 431:263–267

Be'eri-Shlevin Y, Avigad D, Matthews A (2009) Granitoid intrusion and high temperature metamorphism in the Asteroussia Unit, Anafi Island (Greece): petrology and geochronology. Isr J Earth Sci 58:13–27

Bolhar R, Ring U, Allen CM (2010) An integrated zircon geochronological and geochemical investigation into the Miocene plutonic evolution of the Cyclades, Aegean Sea, Greece: part 1: geochronology. Contrib Mineral Petrol 160:719–742

Bonev N, Marchev P, Moritz R, Collings D (2015) Jurassic subduction zone tectonics of the Rhodope Massif in the Thrace region (NE Greece) as revealed by new U–Pb and $^{40}Ar/^{39}Ar$ geochronology of the Evros ophiolite and high-grade basement rocks. Gondwana Res 27:760–775

Bröcker M, Enders M (1999) U–Pb zircon geochronology of unusual eclogite-facies rocks from Syros and Tinos (Cyclades, Greece). Geol Mag 136:111–118

Bröcker M, Franz L (1994) The contact aureole on Tinos (Cyclades, Greece). Part I: field relationships, petrography and P–T conditions. Chem Erde 54:262–280

Bröcker M, Franz L (1998) Rb–Sr isotope studies on Tinos Island (Cyclades, Greece): additional time constraints for metamorphism, extent of infiltration-controlled overprinting and deformational activity. Geol Mag 135:369–382

Bröcker M, Franz L (2000) Contact metamorphism on Tinos (Cyclades, Greece): the importance of tourmaline, timing of the thermal overprint and Sr isotope characteristics. Mineral Petrol 70:257–283

Bröcker M, Franz L (2005) The base of the Cycladic blueschist unit on Tinos Island (Greece) re-visited: field relationships, phengite

chemistry and Rb–Sr geochronology. N Jahrb Mineral Abh 181:81–93

Bröcker M, Keasling A (2006) Ionprobe U–Pb zircon ages from the high-pressure/low-temperature mélange of Syros, Greece: age diversity and the importance of pre-Eocene subduction. J Metamorph Geol 24:615–631

Bröcker M, Pidgeon RT (2007) Protolith ages of meta-igneous and meta-tuffaceous rocks from the Cycladic blueschist unit, Greece: results of a reconnaissance U–Pb zircon study. J Geol 115:83–98

Bröcker M, Kreuzer H, Matthews A, Okrusch M (1993) $^{40}Ar/^{39}Ar$ and oxygen isotope studies of polymetamorphism from Tinos Island, Cycladic blueschist belt. J Metamorph Geol 11:223–240

Bröcker M, Baldwin S, Arkudas R (2013) The geologic significance of $^{40}Ar/^{39}Ar$ and Rb–Sr white mica ages from Syros and Sifnos, Greece: a record of continuous (re)crystallization during exhumation? J Metamorph Geol 31:629–646

Bröcker M, Löwen K, Rodionov N (2014) Unraveling protolith ages of meta-gabbros from Samos and the Attic-Cycladic crystalline belt, Greece: results of a U–Pb zircon and Sr–Nd whole rock study. Lithos 198–199:234–248

Bröcker M, Huyskens M, Berndt J (2015) U–Pb dating of detrital zircons from Andros, Greece: constraints for the time of sediment accumulation in the northern part of the Cycladic blueschist belt. Geol J. doi:10.1002/gj.2634

Bulle F, Bröcker M, Gärtner C, Keasling A (2010) Geochemistry and geochronology of HP mélanges from Tinos and Andros, Cycladic blueschist belt, Greece. Lithos 117:61–81

Candan O, Dora OÖ, Oberhänsli R, Oelsner FC, St Dürr (1997) Blueschist relics in the Mesozoic series of the Menderes Massif and correlation with Samos Island, Cyclades. Schweiz Miner Petrog 77:95–99

Chatzaras V, Dörr W, Finger F, Xypolias P, Zulauf G (2013) U–Pb single zircon ages and geochemistry of metagranitoid rocks in the Cycladic Blueschists (Evia Island): implications for the Triassic tectonic setting of Greece. Tectonophysics 595–596:125–139

Dörr W, Zulauf G, Gerdes A, Lahayec Y, Kowalczyk G (2015) A hidden Tonian basement in the eastern Mediterranean: age constraints from U–Pb data of magmatic and detrital zircons of the External Hellenides (Crete and Peloponnesus). Precambrian Res 258:83–108

Dürr S, Altherr R, Keller J, Okrusch M, Seidel E (1978) The median Aegean crystalline belt: stratigraphy, structure, metamorphism, magmatism. In: Closs H, Roeder DH, Schmidt K (eds) Alps, Apennines, Hellenides. IUGS report no. 38, Schweizerbart, Stuttgart, pp 455–477

Engel M, Reischmann T (1998) Single zircon geochronology of orthogneisses from Paros, Greece. Bull Geol Soc Greece 32:91–99

Feenstra A (1985) Metamorphism of bauxites on Naxos, Greece. Ph.D. Thesis, University of Utrecht, Geologica Ultraiectina 39

Forster MA, Lister GS (2005) Several distinct tectono-metamorphic slices in the Cycladic eclogite-blueschist belt, Greece. Contrib Mineral Petrol 150:523–545

Fu B, Valley JW, Kita NT, Spicuzza MJ, Paton C, Tsujimori T, Bröcker M, Harlow GE (2010) Multiple origins of zircons in jadeitite. Contrib Mineral Petrol 159:769–780

Fu B, Paul B, Cliff J, Bröcker M, Bulle F (2012) O-Hf isotope constraints on the origin of zircon in high-pressure mélange blocks and associated matrix rocks from Tinos and Syros, Greece. Eur J Mineral 24:277–287

Fu B, Bröcker M, Ireland T, Holden P, Kinsley LPJ (2015) Zircon U–Pb, O, and Hf isotopic constraints on Mesozoic magmatism in the Cyclades, Aegean Sea, Greece. Int J Earth Sci 104:75–87

Gärtner C, Bröcker M, Strauss H, Farber F (2011) Strontium, carbon and oxygen isotope geochemistry of marbles from the Cycladic blueschist belt, Greece. Geol Mag 148:511–528

Gehrels G (2011) Detrital zircon U–Pb geochronology: current methods and new opportunities. In: Busby C, Azor A (eds) Tectonics of sedimentary basins: recent advances. Wiley, New York, pp 47–62

Henjes-Kunst F, Kreuzer H (1982) Isotopic dating of pre-Alpidic rocks from the Island of Ios (Cyclades, Greece). Contrib Mineral Petrol 80:245–253

Himmerkus F, Reischmann T, Kostopoulos D (2006) Late Proterozoic and Silurian basement units within the Serbo-Macedonian Massif, northern Greece: the significance of terrane accretion in the Hellenides. In: Robertson AHF, Mountrakis D (eds) Tectonic development of the Eastern Mediterranean Region, vol 260. Geological Society of London Special Publications, pp 35–50

Himmerkus F, Anders B, Reischmann T, Kostopoulos D (2007) Gondwana-derived terranes in the northern Hellenides. In: Hatcher RD Jr, Carlson MP, McBride JH, Martínez Catalán JR (eds) 4-D Framework of continental crust, vol 200. Geological Society of America Memoirs, pp 379–390

Himmerkus F, Reischmann T, Kostopoulos D (2009a) Triassic rift-related metagranites in the Internal Hellenides, Greece. Geol Mag 146:252–265

Himmerkus F, Reischmann T, Kostopoulos D (2009b) Serbo-Macedonian revisited: a Silurian basement terrane from northern Gondwana in the Internal Hellenides, Greece. Tectonophysics 473:20–35

Himmerkus F, Zachariadis P, Reischmann T, Kostopoulos D (2012) The basement of the Mount Athos peninsula, northern Greece: insights from geochemistry and zircon ages. Int J Earth Sci 101:1467–1485

Huet B, Labrousse L, Monié P, Malvoisin B, Jolivet L (2015) Coupled phengite ^{40}Ar–^{39}Ar geochronology and thermobarometry: P–T–t evolution of Andros Island (Cyclades, Greece). Geol Mag 152:711–727

Huyskens M, Bröcker M (2014) The status of the Makrotantalon Unit (Andros, Greece) within the structural framework of the Attic-Cycladic crystalline belt. Geol Mag 151:430–446

Jackson S, Pearson NJ, Griffin WL, Belousova EA (2004) The application of laser ablation-inductively coupled plasma-mass spectrometry to in situ U–Pb zircon geochronology. Chem Geol 211:47–69

Jolivet L, Brun JP (2010) Cenozoic geodynamic evolution of the Aegean. Int J Earth Sci 99:109–138

Jolivet L, Lecomte E, Huet B, Denèle Y, Lacombe O, Labrousse L, Le Pourhiet L, Mehl C (2010) The north Cycladic detachment system. Earth Planet Sci Lett 289:87–104

Katzir Y, Matthews A, Garfunkel Z, Schliestedt M (1996) The tectono-metamorphic evolution of a dismembered ophiolite (Tinos, Cyclades, Greece). Geol Mag 133:237–254

Keay S (1998) The geological evolution of the Cyclades, Greece: constraints from SHRIMP U–Pb geochronology. Dissertation, Australian National University, Canberra

Keay S, Lister G (2002) African provenance for the metasediments and metaigneous rocks of the Cyclades, Aegean Sea, Greece. Geology 30:235–238

Keay S, Lister G, Buick I (2001) The timing of partial melting, Barrovian metamorphism and granite intrusion in the Naxos metamorphic core complex, Cyclades, Aegean Sea, Greece. Tectonophysics 342:275–312

Keiter M, Ballhaus C, Tomaschek F (2011) A new geological map of the Island of Syros (Aegean Sea, Greece): implications for lithostratigraphy and structural history of the Cycladic Blueschist Unit. Geol Soc Am Spec Pap 481:43p

Kneuker T, Dörr W, Petschick R, Zulauf G (2015) Upper crustal emplacement and deformation of granitoids inside the Uppermost Unit of the Cretan nappe stack: constraints from U–Pb zircon dating, microfabrics and paleostress analyses. Int J Earth Sci 104:351–367

Kooijman E, Berndt J, Mezger K (2012) U–Pb dating of zircon by laser ablation ICP-MS: recent improvements and new insights. Eur J Mineral 24:5–21

Koralay OE, Satir M, Dora OO (2001) Geochemical and geochronological evidence for Early Triassic calc-alkaline magmatism in the Menderes Massif, western Turkey. Int J Earth Sci 89:822–835

Kröner A, Sengör AMC (1990) Archean and Proterozoic ancestry in late Precambrian to early Paleozoic crustal elements of southern Turkey as revealed by single zircon dating. Geology 18:1186–1190

Kydonakis K, Kostopoulos D, Poujol M, Brun JP, Papanikolaou D, Paquette JL (2014) The dispersal of the Gondwana Super-fan System in the eastern Mediterranean: new insights from detrital zircon geochronology. Gondwana Res 25:1230–1241

Langosch A, Seidel E, Stosch HG, Okrusch M (2000) Intrusive rocks in the ophiolitic mélange of Crete – witnesses to Late Cretaceous thermal event of enigmatic geological position. Contrib Mineral Petrol 139:339–355

Liati A (2005) Identification of repeated Alpine (ultra) high-pressure metamorphic events by U–Pb SHRIMP geochronology and REE geochemistry of zircon: the Rhodope zone of Northern Greece. Contrib Mineral Petrol 150:608–630

Liati A, Gebauer D, Wysoczanski R (2002) U–Pb SHRIMP-dating of zircon domains from UHP mafic rocks in the Rhodope zone (N Greece); evidence for Early Cretaceous crystallization and Late Cretaceous metamorphism. Chem Geol 184:281–300

Liati A, Gebauer D, Fanning M (2004) The age of ophiolitic rocks of the Hellenides (Vourinos, Pindos, Crete); first U–Pb ion microprobe (SHRIMP) zircon ages. Chem Geol 207:171–188

Liati A, Skarpelis N, Pe-Piper G (2009) Late Miocene magmatic activity in the Attic-Cycladic Belt of the Aegean (Lavrion, SE Attica, Greece): implications for the geodynamic evolution and timing of ore deposition. Geol Mag 146:732–742

Liati A, Gebauer D, Fanning CM (2011) Geochronology of the Alpine (U)HP Rhodope zone: a review of isotopic ages and constraints on the geodynamic evolution. In: Dobrzhinetskaya L, Faryad SW, Wallis S, Cuthbert S (eds) Ultra high-pressure metamorphism, 25 years after the discovery of coesite and diamond. Elsevier, Amsterdam, pp 295–324

Liati A, Skarpelis N, Fanning CM (2013) Late Permian–Early Triassic igneous activity in the Attic Cycladic Belt (Attica): new geochronological data and geodynamic implications. Tectonophysics 595–596:140–147

Lode S, Zulauf G, Dörr W, Fiala J, Lahaye V, Xypolias P (2008) Triassic (Cimmerian) orogenic processes in the External Hellenides - Kythira, Greece: new age constraints from radiometric dating of felsic orthogneiss. Geotectonic Res 95:102–104

Löwen K, Bröcker M, Berndt J (2015) Depositional ages of clastic metasediments from Samos and Syros, Greece: results of a detrital zircon study. Int J Earth Sci 104:205–220

Ludwig KR (2005) Users manual for ISOPLOT/Ex 3.41c: a geochronological toolkit for Microsoft Excel. Berkeley Geochronology Center, Special Publication 4

Marsellos AE, Foster DA, Kamenov GD, Kyriakopoulos K (2012) Detrital zircon U–Pb data from the Hellenic south Aegean belts: constraints on the age and source of the South Aegean basement. J Virt Explorer. doi:10.3809/jvirtex.2011.00284

Meinhold G, Frei D (2008) Detrital zircon ages from the islands of Inousses and Psara, Aegean Sea, Greece: constraints on depositional age and provenance. Geol Mag 145:886–891

Meinhold G, Reischmann T, Kostopoulos D, Lehnert O, Matukov D, Sergeev S (2008) Provenance of sediments during subduction of Palaeotethys: detrital zircon ages and olistolith analysis in Palaeozoic sediments from Chios Island, Greece. Palaeogeogr Palaeoc 263:71–91

Meinhold G, Kostopoulos D, Reischmann T, Frei D, BouDagher-Fadel MK (2009) Geochemistry, provenance and stratigraphic age of metasedimentary rocks from the eastern Vardar suture zone, northern Greece. Palaeogeogr Palaeoc 277:199–225

Meinhold G, Kostopoulos D, Frei D, Himmerkus F, Reischmann T (2010) U–Pb LA-SF-ICP-MS zircon geochronology of the Serbo-Macedonian Massif, Greece: palaeotectonic constraints for Gondwana-derived terranes in the Eastern Mediterranean. Int J Earth Sci 99:813–832

Meinhold G, Morton AC, Avigad D (2013) New insights into peri-Gondwana paleogeography and the Gondwana super-fan system from detrital zircon U–Pb ages. Gondwana Res 23:661–665

Melidonis NG (1980) The geological structure and mineral deposits of Tinos island (Cyclades, Greece). The Geology of Greece 13:1–80

Nance D (2010) Neogene–Recent extension on the eastern flank of Mount Olympus, Greece. Tectonophysics 488:282–292

Okay AI, Satir M, Tüysüz O, Akyüz S, Chen F (2001) The tectonics of the Strandja Massif: late-Variscan and mid-Mesozoic deformation and metamorphism in the northern Aegean. Int J Earth Sci 90:217–233

Okay AI, Tüysüz O, Satir M, Özkan-Altiner S, Altiner D, Sherlock S, Eren RE (2006) Cretaceous and Triassic subduction-accretion, HP–LT metamorphism and continental growth in the Central Pontides, Turkey. Geol Soc Am Bull 118:1247–1269

Okrusch M, Bröcker M (1990) Eclogite facies rocks in the Cycladic blueschist belt, Greece: a review. Eur J Mineral 2:451–478

Papanikolaou D (1978) Contribution to the geology of the Aegean Sea; the island of Andros. Ann Geol Pays Hell 29:477–553

Parlak O, Delaloye M (1999) Precise $^{40}Ar/^{39}Ar$ ages from the metamorphic sole of the Mersin Ophiolite (southern Turkey). Tectonophysics 301:145–158

Parlak O, Karaoğlan F, Rizaoğlu T, Klötzli U, Koller F, Billor Z (2013) U–Pb and 40Ar–39Ar geochronology of the ophiolites and granitoids from the Tauride belt: implications for the evolution of the Inner Tauride suture. J Geodyn 65:22–37

Patzak M, Okrusch M, Kreuzer H (1994) The Akrotiri unit on the island of Tinos, Cyclades, Greece: witness to a lost terrane of Late Cretaceous age. Neues Jahrb Geol Paläontol Abh 194:211–252

Pe-Piper G, Piper DJW (2002) The igneous rocks of Greece: the anatomy of an orogen. Gebrüder Borntraeger, Stuttgart

Photiades A, Keay S (2003) Geological and geochronological data for Sikinos and Folegandros metamorphic units (Cyclades, Greece): their tectono-stratigraphic significance. Bull Geol Soc Greece 35:34–45

Reinecke T, Altherr R, Hartung B, Hatzipangiotou K, Kreuzer H, Harre W, Klein H, Keller J, Geenen E, Boeger H (1982) Remnants of a Late-Cretaceous high-temperature belt on the island of Anafi (Cyclades, Greece). N Jb Miner Abh 145:157–182

Reischmann T (1998) Pre-Alpine origin of tectonic units from the metamorphic complex of Naxos, Greece, identified by single zircon Pb/Pb dating. Bull Geol Soc Greece 32:101–111

Reischmann T, Kostopoulos DK, Loos S, Anders B, Avgerinas A, Sklavounos SA (2001) Late Paleozoic magmatism in the basement rocks southwest of the Mt. Olympos, Central Pelagonian Zone, Greece: remnants of a Permo-Carboniferous magmatic arc. Bull Geol Soc Greece 25:985–993

Ring U, Glodny J, Will T, Thomson S (2010) The Hellenic subduction system: high-pressure metamorphism, exhumation, normal faulting, and large-scale extension. Annu Rev Earth Planet Sci 38:45–76

Robertson AHF (2002) Overview of the genesis and emplacement of Mesozoic ophiolites in the Eastern Mediterranean. Lithos 65:1–67

Schenker FL, Burg J-P, Kostopoulos D, Moulas E, Larionov A, von Quadt A (2014) From Mesoproterozoic magmatism to collisional Cretaceous anatexis: tectonomagmatic history of the Pelagonian Zone, Greece. Tectonics 33:1552–1576

Schermer ER, Lux DR, Burchfiel C (1990) Temperature-time history of subducted continental crust, Mount Olympos region, Greece. Tectonics 9:1165–1195

Schliestedt M, Altherr R, Matthews A (1987) Evolution of the Cycladic crystalline complex: petrology, isotope geochemistry and geochronology. In: Helgeson HC (ed) Chemical transport in metasomatic processes. Reidel Publishing Company, NATO ASI series, pp 389–428

Shaked Y, Avigad D, Garfunkel Z (2000) Alpine high-pressure metamorphism at the Almyropotamos window (southern Evia, Greece). Geol Mag 137:367–380

Stacey JS, Kramers JD (1975) Approximation of terrestrial lead isotope evolution by a two-stage model. Earth Planet Sci Lett 26:207–221

Steiger RH, Jäger E (1977) Subcommission on geochronology: convention on the use of decay constants in geo- and cosmochronology. Earth Planet Sci Lett 36:359–362

Stolz J, Engi M, Rickli M (1997) Tectonometamorphic evolution of SE Tinos, Cyclades, Greece. Schweiz Miner Petrogr Mitt 77:209–231

Tomaschek F, Kennedy AK, Villa IM, Lagos M, Ballhaus C (2003) Zircons from Syros, Cyclades, Greece—recrystallization and mobilization of zircon during high-pressure metamorphism. J Petrol 44:1977–2002

Tomaschek F, Keiter M, Kennedy AK, Ballhaus C (2008) Pre-Alpine basement within the Northern Cycladic Blueschist Unit on Syros Island, Greece. Z dtsch Ges Geowiss 159:521–532

Turpaud P, Reischmann T (2010) Characterisation of igneous terranes by zircon dating: implications for UHP occurrences and suture identification in the Central Rhodope, northern Greece. Int J Earth Sci 99:567–591

Ustaömer PA, Ustaömer T, Gerdes A, Zulauf G (2011) Detrital zircon ages from Ordovician quartzites of the İstanbul exotic terrane (NW Turkey): evidence for Amazonian affinity. Int J Earth Sci 100:23–41

Ustaömer PA, Ustaömer T, Robertson AHF (2012) Ion probe U–Pb dating of the Central Sakarya basement: a peri-Gondwana terrane intruded by Lower Carboniferous subduction/collision-related granitic rocks. Turk J Earth Sci 21:905–932

Vavassis I, De Bono A, Stampfli GM, Giorgis D, Valloton A, Amelin Y (2000) U–Pb and Ar–Ar geochronological data from the Pelagonian basement in Evia (Greece): geodynamic implications for the evolution of Paleotethys. Schweiz Miner Petrogr Mitt 80:21–43

von Quadt A, Moritz R, Peytcheva I, Heinrich C (2005) Geochronology and geodynamics of late Cretaceous magmatism and Cu–Au mineralization in the Panagyurishte region of the Apuseni–Banat–Timok–Srednogorie belt, Bulgaria. Ore Geol Rev 27:95–126

Wiedenbeck M, Allé P, Corfu F, Griffin WL, Meier M, Oberli F, von Quadt A, Roddick JC, Spiegel W (1995) Three natural zircon standards for U–Th–Pb, Lu–Hf, trace element and REE analyses. Geostand Newsl 19:1–23

Xypolias P, Dörr W, Zulauf G (2006) Late Carboniferous plutonism within the pre-Alpine basement of the External Hellenides (Kithira, Greece): evidence from U–Pb zircon dating. J Geol Soc London 163:539–547

Zeffren S, Avigad D, Heimann A, Gvirtznan Z (2005) Age resetting of hanging wall rocks above a low-angle detachment fault: Tinos Island (Aegean Sea). Tectonophysics 400:1–25

Zlatkin O, Avigad D, Gerdes A (2013) Evolution and provenance of Neoproterozoic basement and Lower Paleozoic siliciclastic cover of the Menderes Massif, Western Taurides: coupled U–Pb–Hf zircon isotope geochemistry. Gondwana Res 23:682–700

Zlatkin O, Avigad D, Gerdes A (2014) Peri-Amazonian provenance of the Proto-Pelagonian basement (Greece), from zircon U–Pb geochronology and Lu–Hf isotopic geochemistry. Lithos 184–187:379–392

Zulauf G, Romano SS, Dörr W, Fiala J (2007) Crete and the Minoan terranes: age constraints from U–Pb dating of detrital zircons. Geol Soc Am Spec Papers 423:401–411